



A Journal of the Gesellschaft Deutscher Chemiker

# Angewandte Chemie

GDCh

International Edition

www.angewandte.org

## Accepted Article

**Title:** Ultrahigh-loading Zn Single-atom Catalyst for Highly Efficient Oxygen Reduction Reaction in both Acidic and Alkaline Media

**Authors:** Jia Li, Siguo Chen, Na Yang, Mingming Deng, Shumaila Ibraheem, Jianghai Deng, Jing Li, Li Li, and Zidong Wei

This manuscript has been accepted after peer review and appears as an Accepted Article online prior to editing, proofing, and formal publication of the final Version of Record (VoR). This work is currently citable by using the Digital Object Identifier (DOI) given below. The VoR will be published online in Early View as soon as possible and may be different to this Accepted Article as a result of editing. Readers should obtain the VoR from the journal website shown below when it is published to ensure accuracy of information. The authors are responsible for the content of this Accepted Article.

**To be cited as:** *Angew. Chem. Int. Ed.* 10.1002/anie.201902109  
*Angew. Chem.* 10.1002/ange.201902109

**Link to VoR:** <http://dx.doi.org/10.1002/anie.201902109>  
<http://dx.doi.org/10.1002/ange.201902109>

## COMMUNICATION

# Ultrahigh-loading Zn Single-atom Catalyst for Highly Efficient Oxygen Reduction Reaction in both Acidic and Alkaline Media

Jia Li, Siguo Chen\*, Na Yang, Mingming Deng, Shumaila Ibraheem, Jianghai Deng, Jing Li, Li Li\*, and Zidong Wei\*

**Abstract:** Atomically dispersed Zn-N-C nanomaterials are promising Pt-free catalysts for oxygen reduction reaction (ORR). However, the fabrication of high Zn loading Zn-N-C catalyst remains a formidable challenge due to the high volatility of Zn precursor during high-temperature annealing. Here, we report that the atomically dispersed Zn-N-C catalyst with an ultrahigh Zn loading of 9.33 wt% can be successfully prepared by simply adopting a very low annealing rate of 1°/min. The Zn-N-C catalyst exhibits comparable ORR activity with Fe-N-C catalyst, and significantly better ORR stability than Fe-N-C catalyst in both acidic and alkaline media. Further experiments and DFT calculations demonstrate that Zn-N-C catalyst is less susceptible to protonate than Fe-N-C catalyst in acidic medium. DFT calculations reveal that the Zn-N<sub>4</sub> structure is more electrochemically stable than the Fe-N<sub>4</sub> during ORR process.

Oxygen reduction reaction (ORR) plays a paramount role in a variety of energy conversion and storage systems such as fuel cells and metal-air batteries.<sup>[1]</sup> Atomically dispersed transition metal (M) and N co-doped carbon materials (M-N-C) are emerging as very promising Pt-free ORR catalysts,<sup>[2]</sup> where M and N atoms could induce uneven charge distribution and thus improve the O<sub>2</sub> adsorption and reduction.<sup>[3]</sup> The best M-N-C catalyst developed so far has a high initial activity with turnover frequencies matching those of Pt/C;<sup>[4]</sup> However, their practical use was impeded by the unsatisfactory physical and chemical stability.<sup>[5]</sup> Moreover, the reported transition metal sources are mainly limited to the Fe, Co, Ni and Mn.<sup>[6]</sup> It has been proven that residues of these transition metals, i.e. Fe<sup>2+</sup> or Fe<sup>3+</sup> (intermediate valence of transition metals), and some incompletely coordinated ions, can deteriorate the stability of the electrode and electrolyte membrane during ORR.

Compared with Fe, Co, Ni and Mn, the element Zn has a full-filled d orbital (3d<sub>10</sub>4s<sub>2</sub>), thus cannot form oxidative ions with a high valence state. Therefore, it is expected that Zn-N-C catalyst would be harmless to the electrode and electrolyte membrane. Unfortunately, the performance of the reported Zn-N-C catalysts in ORR is not as good as Fe-N-C catalysts, which probably can be assigned to the low active site density as listed in **Table S1**. Generally, the fabrication of atomically dispersed Zn-N-C catalyst, while maintaining high density of atomic Zn sites, has been

proved to be difficult.<sup>[7]</sup> This is due to the fact that Zn precursor is easily removed due to its high volatility during high-temperature pyrolysis process.

Herein, we markedly increase the loading of atomically dispersed Zn in Zn-N-C catalysts by strictly controlling the gasification rate of Zn precursor. This route indeed well converts the precursors, ZnCl<sub>2</sub> and ortho-phenylenediamine (oPD) into stable Zn-N<sub>x</sub> active sites before their gasification, and thus achieves a loading of Zn single-atom as high as 9.33 wt% (2.06 atom%). The atomically dispersed Zn-N-C catalyst exhibits not only comparable ORR activity with Fe-N-C catalyst in both acidic and alkaline media, but also better durability than Fe-N-C catalyst. XPS analysis demonstrates that the Zn-N-C-1 (the number “1” represents the heating rate of 1°/min during annealing) catalyst is less susceptible to protonate than Fe-N-C-1 catalyst in acidic medium. Density functional theory (DFT) calculations reveal that the Zn-N<sub>4</sub> structure is more electrochemically stable than the Fe-N<sub>4</sub> structure during ORR process.

An optimal atomically dispersed Zn-N-C catalyst was prepared by pyrolyzing the mixed precursor system of poly o-phenylenediamine (PoPD) and ZnCl<sub>2</sub> at a heating rate of 1°/min (Please see supporting information). The Zn loading of the optimal Zn-N-C-1 catalyst is 9.33 wt% (2.06 atom%) by EDX (energy-dispersive X-ray spectroscopy) method, and 5.64 wt% by ICP-MS (inductively coupled plasma mass spectrometry) analysis, which is much higher than that of Fe-N-C-1 catalyst obtained at the same annealing conditions (**Table S2**). For comparison, the samples pyrolyzed at different annealing rates are also prepared and denoted as Zn-N-C-X (X=annealing rates). The ORR activities of Zn-N-C catalysts were evaluated in both acidic and alkaline solutions by the rotating disk electrode (RDE) and rotating ring-disk electrode (RRDE). As shown in **Figure 1a**, the ORR activity of Zn-N-C in acidic medium increases quickly with the decrease of annealing rate and reaches the most positive half-wave potential of 0.746 V at 1°/min (Zn-N-C-1), which is comparable to the Fe-N-C-1 catalyst (0.743 V). The same trend is also observed in alkaline solution (**Figure 1b**), in which the half-wave potential (0.873V) of the optimal Zn-N-C-1 catalyst is more positive than that of commercial Pt/C catalyst (0.858V), and slightly lower than that of the Fe-N-C-1 catalyst (0.880V). The H<sub>2</sub>O<sub>2</sub> yield of Zn-N-C-1 catalyst in both acidic and alkaline solutions is less than 5% indicating a four-electron reduction pathway, which is comparable to that of Fe-N-C-1 catalyst (**Figure S1**).

In order to understand the origin of the observed high ORR activity of Zn-N-C-1 catalyst, a series of physical characterizations has been carried out. The dominant diffraction peaks of Zn-N-C-1 catalyst in the X-ray diffraction (XRD) pattern are consistent with the partially graphitized carbon structures (**Figure S2**), which is confirmed by high-resolution transition electron microscopy (HRTEM) image (**Figure 1c**).<sup>[8]</sup> Both XRD patterns and HRTEM image verify the absence of any visible Zn-based particles or

[\*] Dr. J. Li, Prof. G. S. Chen, Prof. L. Li, Prof. D. Z. Wei  
Chongqing Key Laboratory of Chemical Process for Clean Energy  
and Resource Utilization, School of Chemistry and Engineering,  
Chongqing University  
Shazhengjie 174, Chongqing 400044 (China)  
E-mail: csg810519@126.com  
liliracial@cqu.edu.cn  
zdwei@cqu.edu.cn

Supporting information for this article is given via a link at the end of the document.

## COMMUNICATION

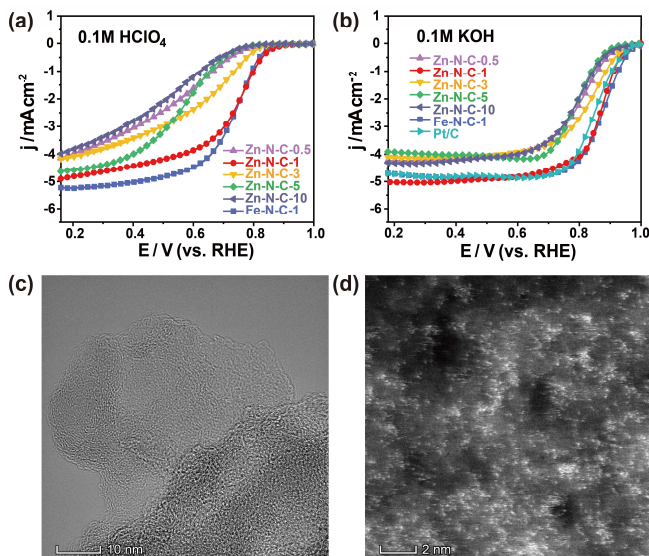


**Figure 1.** ORR polarization curves of Zn-N-C-X and Fe-N-C-X catalysts (X=annealing rates, 0.5°/min, 1°/min, 3°/min, 5°/min 10°/min) recorded in O<sub>2</sub>-saturated 0.1 M HClO<sub>4</sub> (a) and 0.1 M KOH solution (b) at room temperature with a sweep rate of 10 mV s<sup>-1</sup> and a rotation rate of 1600 rotations min<sup>-1</sup>. (c) The HRTEM image of Zn-N-C-1 catalyst. (d) The aberration-corrected HAADF-STEM image of Zn-N-C-1 catalyst (single-atom Zn are the bright dots).

clusters in Zn-N-C-1 catalyst. To illustrate the existence state of the Zn species, aberration-corrected atomic-resolution HAADF-STEM measurement has been carried out,<sup>[9]</sup> which clearly shows that Zn single-atoms are uniformly dispersed in Zn-N-C-1 sample at a very high density because the atomic number of Zn is much higher than the support elements (Figure 1d). By counting the amount of Zn single-atoms in the special area in Figure S3, the density of Zn single-atom can be roughly estimated to be 9.31 atoms/nm<sup>2</sup>, which is indeed among the highest ones in all reported single-atom catalysts (Table S1). The corresponding Zn content obtained by EDX is about 9.33 wt% (2.06 at%) (Figure S4), which is very close to the value of 2.47 at% determined by XPS (Table S2), and larger than 5.64 wt% determined by ICP-MS (Table S2 and Figure S5). Moreover, we found that a lower heating rate of 0.5°/min cannot accomplish the conversion of ZnCl<sub>2</sub> into Zn-N-C catalyst (Table S2 and Figure S6). This is because at such a low heating rate, PoPD precursor, after being held at low-temperatures for a long time, would preferentially transform into amorphous carbon, which while cannot capture Zn species to form atomic Zn doping. That is why the Zn-N-C-0.5 catalyst shows significantly reduced activity compared to the Zn-N-C-1 catalyst.

The valence state and coordination environment of the atomic Zn of Zn-N-C-1 catalyst are further determined by X-ray absorption near-edge structure (XANES) spectroscopy and extended X-ray absorption fine structure (EXAFS) spectroscopy analysis.<sup>[10]</sup> As shown in Zn K-edge XANES spectra (Figure 2a), the position of absorption threshold for Zn-N-C-1 is close to ZnO and ZnPc, indicating that the valence state of zinc species in Zn-N-C-1 is probably situated +2. The Fourier transforms of EXAFS spectra (FT-EXAFS, without phase correction) in Figure 2b reveal that Zn-N-C-1 exhibits similar Zn-N coordination with a

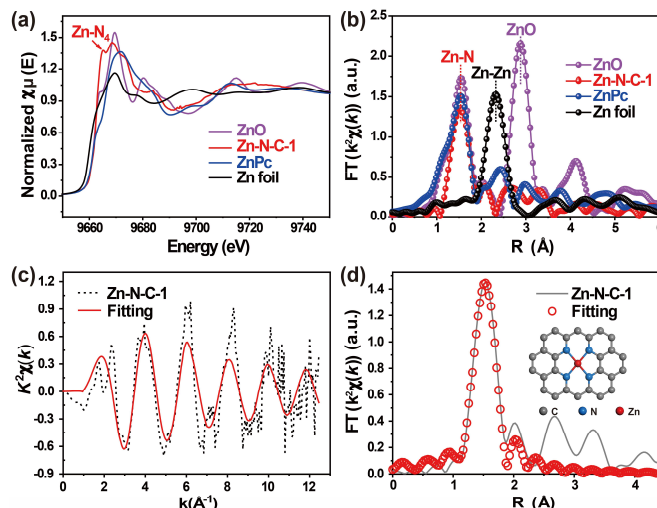


**Figure 2.** (a) Zn K-edge XANES spectra of Zn-N-C-1, ZnO, ZnPc, and Zn foil. (b) Fourier transformed (FT)  $k^2$ -weighted  $\chi(k)$ -function of the EXAFS spectra for Zn K-edge. (c, d) Corresponding EXAFS fitting curves at  $k$  and  $R$  space, respectively, inset showing the schematic model.

peak at about 1.53 Å. Meanwhile, metallic signal peaks of Zn-Zn interactions in Zn foil and ZnO were not detected in Zn-N-C-1, manifesting that the Zn element is atomically dispersed in the Zn-N-C-1 catalyst. The best fitting result of the obtained EXAFS data reveals that Zn-N<sub>4</sub> rather than Zn-Zn/Zn-N<sub>2</sub> coordination structure is the dominant coordination mode of Zn atoms in Zn-N-C-1 (Figure 2c, Figure 2d, Table S3). This result clearly indicates that the Zn-N-C-1 catalyst is actually a Zn single-atom catalyst with Zn-N<sub>4</sub> structure. The formation of Zn-N<sub>x</sub> structure is also confirmed by the high-resolution XPS (Figure S7, S8, Table S4).

The pore-making ability of ZnCl<sub>2</sub> was also investigated by scanning electron microscopy (SEM), HRTEM, and N<sub>2</sub> adsorption-desorption tests. As revealed by SEM images (Figure S9a and S9b), Zn-N-C-1 catalyst shows typical interconnected 3D macroporous networks, and no 3D macropore can be found in N-C catalyst obtained with the absence of ZnCl<sub>2</sub>. The average diameter of the macropores is over 500 nm (Figure S9a). The HRTEM image shows that a large quantity of micropores and small size mesopores surround the graphitic layers in the edge regions of Zn-N-C-1 (Figure 1c). The lattice fringe spacing of around 0.34 nm (Figure S10) agrees well with that of graphite. The corresponding Raman spectrum analysis (Figure S11) shows that the ratio of the relative intensity of the D band at 1340 cm<sup>-1</sup> to the G band at 1590 cm<sup>-1</sup> ( $I_D/I_G$ ) for Zn-N-C-1 is lower than that of N-C-1 catalyst, suggesting that the presence of ZnCl<sub>2</sub> not only benefits the formation of micro-/meso-/macro-pores, but also ensures a higher graphitization degree. The Brunauer-Emmett-Teller (BET) specific surface area of Zn-N-C-1 was measured to be 1002 m<sup>2</sup> g<sup>-1</sup> (Figure S12), which is much larger than that of N-C-1 (81 m<sup>2</sup> g<sup>-1</sup>), further confirming that the existence of ZnCl<sub>2</sub> results in the formation of micro-/meso-/macro-pores. By comparing the N<sub>2</sub> adsorption-desorption results, we found that tuning heating rates will not significantly change BET specific surface areas for the Zn-N-C-X samples. Obviously, such multimodal porous structure with well-balanced macro-/meso-/

## COMMUNICATION

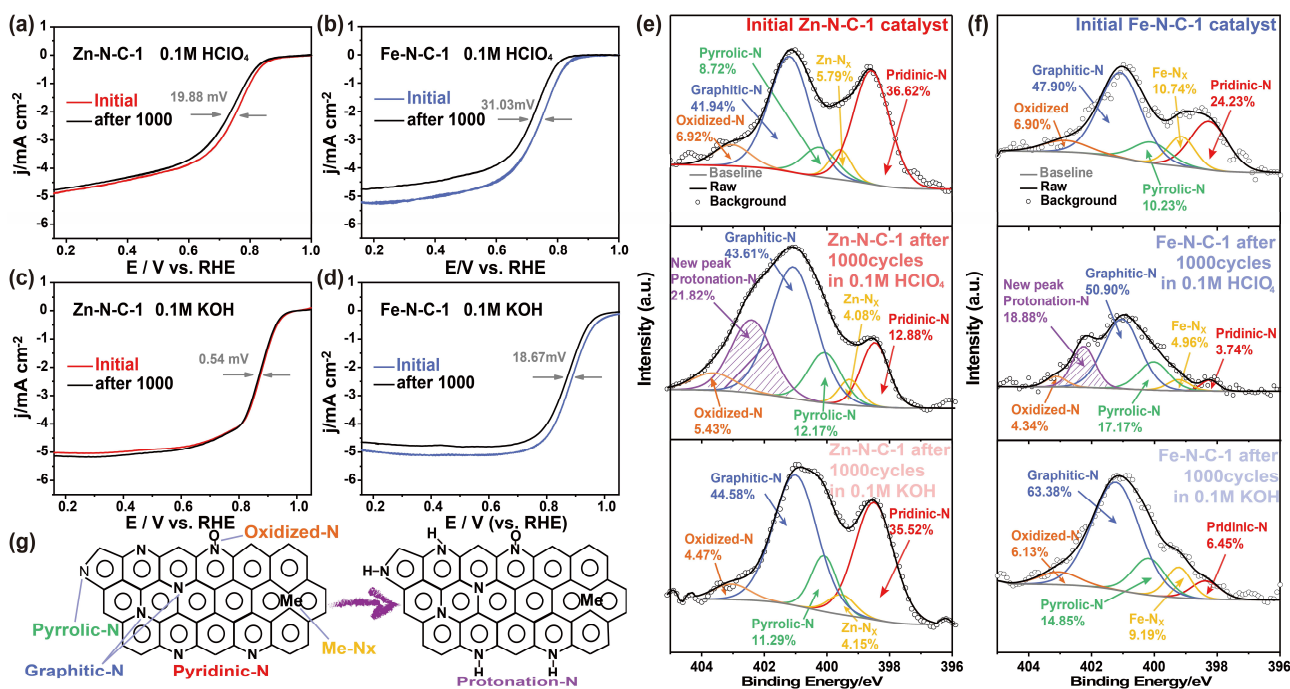


**Figure 3.** The ORR polarization of Zn-N-C-1 and Fe-N-C-1 catalysts before, and after 1000 cycles between 0.6 and 1.1 V versus RHE in 0.1 M HClO<sub>4</sub> (a, c) and 0.1 M KOH (b, d) solutions. High-resolution of N1s spectra of Zn-N-C-1 (e) and Fe-N-C-1 (f) catalysts before, and after 1000 cycles between 0.6 and 1.1 V versus RHE in 0.1 M HClO<sub>4</sub> and 0.1 M KOH solutions. (g) Schematic of the protonation reaction on Zn-N-C-1 and Fe-N-C-1 in acidic solutions.

micro-porosities, high graphitization degree and high surface area could partially explain the high activity of Zn-N-C-1, because: 1) the high specific surface area hosts enormous active-sites for ORR; 2) the high graphitization degree of carbon allows smooth electron transfer; 3) the interconnected 3D macroporous networks guarantee rapid mass exchanges during ORR process.

Since catalyst durability is extremely significant for practical use of Zn-N-C catalyst, we investigated the ORR durability of Zn-N-C-1 and Fe-N-C-1 catalysts in accelerated stress tests (AST) in both acidic and alkaline media. As shown in **Figure 3a**, the half-wave potential of Zn-N-C-1 catalyst decays only 19.88 mV after 1000 CV cycles between 0.6 and 1.1 V in the O<sub>2</sub>-saturated 0.1 M HClO<sub>4</sub>, which is much less than that of Fe-N-C-1 catalyst (31.03 mV) (**Figure 3b**). The Zn-N-C-1 catalyst also exhibits excellent stability in alkaline media, as evidenced by no obvious change in half-wave potential after 1000 CV cycles (**Figure 3c**). By contrast, the Fe-N-C-1 catalyst shows 18.67 mV fading of half-wave potentials in alkaline media (**Figure 3d**). These results suggest that Zn-N-C-1 catalyst is more electrochemically stable than the Fe-N-C-1 catalyst in both acidic and alkaline solutions.

To deeply understand the origin of the observed high durability of Zn-N-C-1 catalyst, the XPS measurements were adopted to monitor the changes of N configurations for Zn-N-C-1 and Fe-N-C-1 electrodes before and after AST tests (**Figure S13, Table S4**). As shown in **Figure 3e** and **3f**, the high-resolution N1s spectra of pristine Zn-N-C-1 and Fe-N-C-1 electrodes can be deconvoluted into five peaks associated with the pyridinic-N (398.4 eV), Zn(or Fe)-N<sub>x</sub> (≈399.6 eV), pyrrolic-N (400.2 eV), graphitic-N (401.2 eV), and oxidized-N, (403-405 eV).<sup>[11]</sup> After

1000 CV cycles in acidic medium, a new peak associated with the protonation of pyridinic-N arised at approximately 401.4 eV (protonation-pyridinic-N) for both Zn-N-C-1 and Fe-N-C-1 catalysts. By comparing the atomic percentages of pyridinic-N before and after AST, one can find that both Zn-N-C-1 and Fe-N-C-1 catalysts experienced protonation in acidic medium. However, the Zn-N-C-1 catalyst exhibits a relatively small decrease in pyridinic-N content from 36.62% to 12.88% as compared with the Fe-N-C-1 catalyst from 24.23% to 3.74%. Moreover, we found that the Zn-N-C-1 catalyst largely maintains its Zn-N<sub>x</sub> active sites by showing only a slight decrease in Zn-N<sub>x</sub> content from 5.79% to 4.08% in acidic medium, while the Fe-N-C-1 catalyst shows a rather heavy decrease in Fe-N<sub>x</sub> content from 10.74% to 4.96%. In comparison, both of Zn-N-C-1 and Fe-N-C-1 catalysts largely remain their Zn-N<sub>x</sub> and Fe-N<sub>x</sub> active sites after 1000 CV cycles in alkaline medium, respectively. These results indicate that the Zn-N-C-1 catalyst is less susceptible to protonate than Fe-N-C-1 catalyst in acidic medium, and at the same time, the Zn-N<sub>x</sub> is more stable than the Fe-N<sub>x</sub> in acidic solution.

The protonation effect on the C-N bond stability of the pyridinic-N doped graphene (PNG) and oxidized PNG (PNG-O) was explored by DFT calculations.<sup>[12]</sup> As seen from **Figure 4a**, the bond distances of C1-N in PNG show gradual increase from 1.32 Å to 1.37 Å and 1.45 Å after protonating with one H<sup>+</sup> and two H<sup>+</sup>, respectively. In comparison, the C1-N bond with no protonation in PNG-O (1.44 Å) is much larger than that in PNG (1.32 Å), and this bond will increase to 1.50 Å with one H<sup>+</sup> and then break after protonating with two H<sup>+</sup> (d<sub>C1-N</sub>=1.44 Å - 1.50 Å - break). These results indicate that the protonation of pyridinic-N in PNG with the

## COMMUNICATION

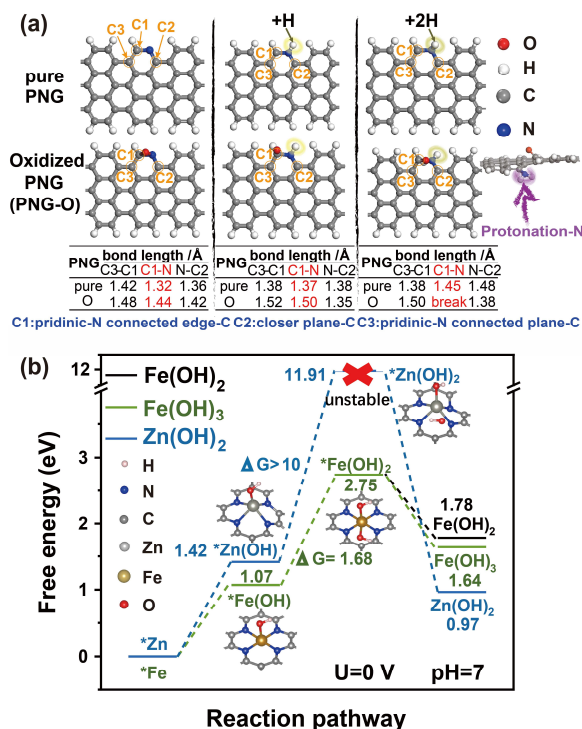


**Figure 4.** (a) DFT-optimized structures of PNG and PNG-O as non-protonated, protonation-H and protonation-2H. (b) Free energy diagrams for the Zn(OH)<sub>2</sub>, Fe(OH)<sub>2</sub> and Fe(OH)<sub>3</sub> during the metal corrosion process based on M-N<sub>4</sub> (M=Zn/Fe) structure.

existence of O<sub>2</sub> will accelerate the breaking of C-N bond, and thus decrease the number of active sites and reduce the ORR activity.

The anti-corrosion ability of Zn-N<sub>4</sub> and Fe-N<sub>4</sub> structures is also evaluated by DFT calculation.<sup>[13]</sup> The OH<sup>-</sup>, which is the ORR intermediate, can adsorb on the metal sites and then oxidize them. Once two OH\* bond to a metal site, the oxidized metal tends to dissociate in the solution. As shown in **Figure 4b**, the free energy transferring Zn site (\*Zn) to \*Zn(OH) is 1.42 eV, which is much larger than the value of 1.07 eV for the formation of \*Fe(OH). Moreover, we found that the formation of \*Zn(OH)<sub>2</sub> from \*Zn(OH) is almost impossible because the free energy is larger than 10 eV. While, the formation of \*Fe(OH)<sub>2</sub> from \*Fe(OH) is feasible due to the low free energy ( $\Delta G = 1.68$  eV). These results indicate that the corrosion of \*Zn site in Zn-N<sub>4</sub> structure is tougher than that of \*Fe site in Fe-N<sub>4</sub> during ORR process. This phenomenon can be attributed to the distinction of valence electron configurations between Fe(3d<sub>6</sub>4s<sub>2</sub>) and Zn(3d<sub>10</sub>4s<sub>2</sub>), in which the Fe site with more d empty orbital tends to adsorb OH<sup>-</sup> and form Fe(OH)<sub>x</sub> species in the ORR process.

Finally, we constructed a Zn-O<sub>2</sub> battery to evaluate the potential of our catalyst for real energy conversion devices (**Figure S14**).<sup>[14]</sup> Commercial Pt/C was also tested under the same conditions for comparison. The maximum power density for Zn-N-C-1 catalyst is 179 mW cm<sup>-2</sup>, slightly higher than that of Pt/C (173 mW cm<sup>-2</sup>) (**Figure S15a**). The potential gaps between Zn-N-C-1 and Pt/C catalysts at different discharge currents were also calculated to give insight into the origin of high activity of the Zn-N-C-1 catalyst. It was found that the potential gaps between Zn-

N-C-1 and Pt/C catalysts dramatically increase from 42.4 mV at 1 mA cm<sup>-2</sup> and 1 mV at 10 mA cm<sup>-2</sup> to 25.7 mV at 100 mA cm<sup>-2</sup> (**Figure S15b**), suggesting that the Zn-N-C-1 catalyst is more conducive to the mass-transfer at higher current densities. The specific capacity was measured according to the consumption of Zn (**Figure S16**). At 100 mA cm<sup>-2</sup>, the Zn-N-C-1 catalyst enabled the Zn-O<sub>2</sub> battery with a specific capacity of 683.3 mAh g<sub>Zn</sub><sup>-1</sup> (about 83.3% utilization of the theoretical capacity 820 mAh g<sub>Zn</sub><sup>-1</sup>), corresponding to a high energy density of 666 Wh kg<sub>Zn</sub><sup>-1</sup> (about 61.3% of the theoretical energy density 1086 Wh kg<sub>Zn</sub><sup>-1</sup>). These values also significantly outperform those of the battery prepared with Pt/C (specific capacity of 601.4 mAh g<sub>Zn</sub><sup>-1</sup> and energy density of 563 Wh kg<sub>Zn</sub><sup>-1</sup>), and even comparable to the best results recently reported for Zn-O<sub>2</sub> batteries (**Table S5**).

In conclusion, we have successfully synthesized ultrahigh loading Zn single-atom catalysts by controlling the annealing rate of ZnCl<sub>2</sub> precursor at 1<sup>o</sup>/min. The XANES and EXAFS experiments reveal that Zn-N<sub>4</sub> is the main active site in Zn-N-C catalyst. Electrochemical experiment tests show that the atomically dispersed Zn-N-C catalyst exhibits not only comparable ORR activity with Fe-N-C catalyst in both acidic and alkaline media, but also better durability than that of Fe-N-C catalyst. XPS analysis demonstrates that the Zn-N-C-1 catalyst is less susceptible to protonate than Fe-N-C-1 catalyst in acidic medium. Meanwhile, DFT calculations reveal that the Zn-N<sub>4</sub> structure is more electrochemical stable than the Fe-N<sub>4</sub> structure during ORR process. This work may represent a new class of high-efficiency and stable single-atom site catalysts for both fundamental research and practical applications.

## Acknowledgements

This work was financially supported by the National Key Research and Development Program of China (2016YFB0101202), and by the National Natural Science Foundation of China (Grant Nos. 21761162015, 91534205, 21436003, 21576031, and 21776023).

**Keywords:** fuel cells • metal-air battery • oxygen reduction reaction • electrocatalyst • Zn single-atom catalyst

- [1] a) M. K. Debe, *Nature* **2012**, *486*, 43-51; b) J. Guo, C. -Y. Lin, Z. Xia, Z. Xiang, *Angew. Chem. Int. Ed.* **2018**, *57*, 12567-12572; c) S. G. Chen, Z. D. Wei, X. Q. Qi, L. C. Dong, Y. G. Guo, L. J. Wan, Z. G. Shao and L. Li, *J. Am. Chem. Soc.* **2012**, *134*, 13252-13255.
- [2] M. Lefèvre, E. Proietti, F. Jaouen, J.-P. Dodelet, *Science* **2009**, *324*, 71-74.
- [3] J. Li, S. Chen, W. Li, R. Wu, S. Ibraheem, J. Li, W. Ding, L. Li, Z. Wei, *J. Mater. Chem. A* **2018**, *6*, 15504-15509.
- [4] X. F. Yang, A. Wang, B. Qiao, J. Li, J. Liu, T. Zhang, *Acc. Chem. Res.* **2013**, *46*, 1740-1748.
- [5] Z. Y. Wu, X. X. Xu, B. C. Hu, H. W. Liang, Y. Lin, L. F. Chen, S. H. Yu, *Angew. Chem.* **2015**, *127*, 8297-8301.
- [6] J. Shui, M. Wang, F. Du, L. Dai, *Sci. Adv.* **2015**, *1*, 1:e1400129.
- [7] P. Song, M. Luo, X. Liu, W. Xing, W. Xu, Z. Jiang, L. Gu, *Adv. Funct. Mater.* **2017**, *27*, 1700802.
- [8] S. H. Ahn, X. Yu, A. Manthiram, *Adv. Mater.* **2017**, *29*, 1606534.
- [9] R. Lang, T. Li, D. Matsumura, S. Miao, Y. Ren, Y. -T. Cui, Y. Tan, B. Qiao, L. Li, A. Wang, X. Wang, T. Zhang, *Angew. Chem. Int. Ed.* **2016**, *55*, 16054-16058.

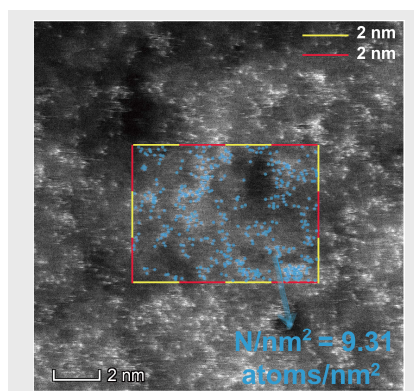
## COMMUNICATION

- [10] T. Sun, S. Zhao, W. Chen, D. Zhai, J. Dong, Y. Wang, S. Zhang, A. Han, L. Gu, R. Yu, X. Wen, H. Ren, L. Xu, C. Chen, Q. Peng, D. Wang, Y. Li, *Pro. Nat. Acad. Sci. USA* **2018**, *115*, 12692-12697.
- [11] W. Ding, Z. Wei, S. Chen, X. Qi, T. Yang, J. -S. Hu, D. Wang, L. -J. Wan, S. Fatima Alvi, L. Li, *Angew. Chem. Int. Ed.* **2013**, *52*, 11755-11759; *Angew. Chem.* **2013**, *125*, 11971-11975.
- [12] T. Sun, L. Xu, D. Wang, Y. Li, *Nano Res.* **2019**, DOI: 10.1007/s12274-019-2345-4.
- [13] P. Zhang, X. F. Chen, J. S. Lian, Q. Jiang, *J. Phys. Chem. C* **2012**, *116*, 17572-17579.
- [14] S. Li, C. Cheng, X. Zhao, J. Schmidt, A. Thomas, *Angew. Chem. Int. Ed.* **2018**, *57*, 1856-1862

## COMMUNICATION

## COMMUNICATION

The atomically dispersed Zn-N-C catalyst with an ultra-high loading of 9.33 wt% Zn single-atom is successfully prepared by decreasing the annealing rate to 1°/min. The Zn-N-C catalyst exhibits comparable ORR activity with Fe-N-C catalyst, and better ORR stability than Fe-N-C catalyst in both acidic and alkaline media.



Jia Li, Siguo Chen\*, Na Yang, Mingming Deng, Shumaila Ibraheem, Jianghai Deng, Jing Li, Li Li\*, and Zidong Wei\*

Page No. – Page No.

**Ultrahigh-loading Zn Single-atom Catalyst for Highly Efficient Oxygen Reduction Reaction in both Acidic and Alkaline Media**

Accepted Manuscript